Comparative Performance of Mitigation Voltage Sag/Swell and Harmonics Using DVR-BES-PV System with MPPT-Fuzzy Mamdani/MPPT-Fuzzy Sugeno

Agus Kiswantono[1]   Eko Prasetyo[2]   Amirullah Amirullah[1*]

[1]Electrical Engineering Study Program Faculty of Engineering,
University of Bhayangkara Surabaya, Surabaya, Indonesia
[2]Informatics Engineering Study Program Faculty of Engineering,
University of Bhayangkara Surabaya, Surabaya, Indonesia
* Corresponding author's Email: amirullah@ubhara.ac.id

Abstract: This paper presents comparative performance between Maximum Power Point Tracking-Fuzzy Mamdani (MPPT-FM) and MPPT-Fuzzy Sugeno (FS) methods as controller on Photovoltaic (PV) output power using Dynamic Voltage Restorer-Battery Energy Storage-PV (DVR-BES-PV) system connected to three phase three wire (3P3W) distribution network. The combination of DVR-BES-PV system using two methods is used in order to mitigate voltage sag/swell and harmonics on load bus. The PV is used as an alternative DC voltage source to charge BES when its capacity decreases and provides active power needed to compensate for sag/swell. In nine sag/swell disturbances scenario, MPPT-FM is able to give better performance in percentage of sag/swell on load voltage than MPPT-FS. In 90% voltage sag, MPPT-FM is able to result percentage of voltage sag on load bus of 5.759% smaller than MPPT-FS of 5.770%. Then, in 190% voltage swell, MPPT-FM is able to result percentage of voltage swell on load bus of 0.892% smaller than MPPT-FS of 1.064%. Both methods are also able to result percentage of sag/swell on load voltage under IEEE 1159. In voltage sag, MPPT-FM is able to result an average Total Harmonics Distortion (THD) of load voltage higher than MPPT-FS. Otherwise in voltage swell, MPPT-FM is able to result an average THD of load voltage smaller than MPPT-FS. In 90% voltage sag, MPPT-FM is able to result average THD of load voltage of 10.32% higher than MPPT-FS of 10.14%. Otherwise, in 190% voltage swell, MPPT-FM is able to result average THD on load bus of 1.594% smaller than MPPT-FS of 2.087%. The average THD of load voltage using MPPT-FM/MPPT-FS in nine voltage swell disturbances scenario on source bus, is smaller than voltage sag and it has met limit of IEEE 519. This research is simulated using Matlab/Simulink environment.

Keywords: MPPT-FM, MPPT-FS, Sag/Swell, Harmonics, THD, DVR, BES, PV.

1. Introduction

The diminishing of fossil energy sources and increasing concerns about environmental impacts have caused renewable energy (RE) sources i.e. PV and wind to develop into alternative energy of power generation. The electrical power produced by PV is direct current (DC), so it requires an inverter before it is operated and connected to distribution system (grid). The disadvantage of PV is beside able to supply power to grid, it also generates harmonics due to presence of voltage source inverter (VSI) type filter as a medium to convert DC to AC

voltage so that it can reduce power quality. On the other hand, with increasing sensitive load penetration, causing power quality problems in modern distribution systems has increased significantly. The most serious and frequent disturbances in grid voltage are sag, swell, and short circuit. The sag is a decrease in rms voltage between 10-90% which lasts from one half cycle to one minute. The swell is an increase in the source rms voltage in a short time interval whose values range from 1.1 pu to 1.8 p.u from nominal source voltage. The device that is capable of effectively and comprehensively overcoming sag/swell disturbance is DVR. Research on sag compensation using DVR

with unit vector template generation (UVTG) method has been done [1]. DVR is able to compensate for balanced and unbalanced sag voltage and inject the desired voltage component to quickly repair a number of interference anomalies at the source voltage to keep load voltage balanced and constant at nominal value.

The comparative analysis of three compensation techniques i.e. phase-by-method compensation, pre-dip compensation method (called large voltage difference compensation), and intelligent phase compensation method has been investigated [2]. A model for DVR control independently has been proposed [3]. The three of three phase harmonics filters (double tuned) were used to mitigate harmonics generated by a voltage source converter (VSC). The low DVR rating was able to compensate for sag, swell, and reduce THD voltage on load bus according to IEEE-519. DVR performance on sag voltage and load voltage harmonics using Sinusoidal Pulse control Width Modulation (SPWM) and Space Vector Pulse Width Modulation (SVPWM) have been done [4]. The Synchronous Reference Frame (SRF) method has been used to detect sag and generate modulation signals. The load voltage THD using the SVPWM method was smaller than SPWM.

The grid integration system connected PV system with self supported DVR has been proposed [5]. The system was called a "six-port converter," whole consists of nine semiconductor switches, reduced from 12 previous semiconductors. The configuration was able to operate in different modes based on grid conditions and PV power. The research were conducted on normal grid mode, interference mode, sag mode, and non-active PV mode. PV based DVR model to overcome sag/swell voltage and outages in single phase low voltage housing distribution systems have been proposed [6]. The simulation shows that DVR-based PV with fuzzy logic controller (FLC) is able to provide better dynamic performance in overcoming voltage variations. DVR was operated in standby, active, bypass, power saver mode. DVR performance to mitigate sag voltage and reduce the THD of load voltage has been investigated [7]. The sag compensation on balanced and unbalanced disturbances conditions with variations in source voltage level sag uses PI and FLC method respectively on series active filter of DVR control. The simulation showed that FLC was able to maintain load voltage constant at nominal value and reduce load voltage THD better than PI.

Efficient FLC based on the power management scheme on the DVR in mitigating a number of voltage disturbances has been proposed [8]. The simulation showed that proposed model was efficiently able to maintain DVR output power below the predetermined value and reduce disturbance according to the priority given. The design and analysis of dynamic FLC on DVR is presented and expanded to perform fast error detection. The combination of DVR control methods using FLC and modulation of PWM carriers in an inverter circuit to detect voltage disturbances quickly has been investigated [9]. The proposed model is able to achieve superior performance for balanced and unbalanced sag/swell voltage mitigation. The start and end times of sag/swell voltage can be quickly detected and without oscillation. Fast switching capabilities can also be used in static transfer switches to improve power system reliability. Analysis of sag/swell voltage compensation using DVR and PV systems supported by energy storage elements (battery) has been carried out [10]. The PV system uses MPPT control with an incremental conductance (IC) algorithm as a RE source, which functions to inject reactive power during disturbance. Otherwise the energy storage (battery) element was used to improve system reliability. Integration of solar PV, battery, and DVR during dynamic disturbance conditions in distribution system has been done [11]. The solar PV system using boost converter was implemented using MPPT with IC algorithm. The PV system was supplied in two ways i.e. to meet load demands and maintain the DC link voltage of DVR in voltage sources converter VSC. The sensitive load and grid voltage were balanced by injecting voltage in series with distribution line. The DVR consists of injection transformers, filter circuits, three-phase series active filters, DC source voltage, and energy storage. The energy storage commonly used is DC-link capacitor. The disadvantage of this device has limited energy storage capacity. In order to overcome these problems, BES supplied by PV is used to mitigate sag/swell and harmonics on low voltage distribution network. This combination is called DVR-BES-PV system and installed on three phase three wire (3P3W) distribution network to maintain voltage on sensitive load. The advantage of BES has a larger storage capacity than capacitor. Moreover, PV is used as an alternative DC voltage source to charge BES when its capacity decreases and provides active power needed to compensate for sag/swell. The UVTG method is used to control series active filter in DVR when it injects compensation voltage during voltage sag/swell disturbance. The PV also helps with the self charging process of the system during uninterrupted condition (standby mode).

Table 1. Abbreviation

Symbol	Description
MPPT	Maximum Power Point Tracking
FM	Fuzzy Mamdani
FS	Fuzzy Sugeno
FIS	Fuzzy Inference System
MFs	Membership Functions
FLC	Fuzzy Logic Controller
THD	Total Harmonics Distortion
DVR	Dynamic Voltage Restorer
BES	Battery Energy Storage
PV	Photovoltaic
RE	Renewable Energy
UVTG	Unit Vector Template Generation
PWM	Pulse With Modulation
3P3W	Three Phase Three Wire
PCC	Point Common Coupling
P and O	Perturb and Observe
IC	Incremental Conductance
AI	Artificial Intelligent

Because of movement of sun, PV panel angle, and irradiance variation reaching the panel, sunlight absorbed and power generated by PV panel is not always constant. If this condition occurs then VI characteristic will change and MPP will move. To overcome this problem, MPPT method has been developed. MPPT is looking for independent maximum power based on environmental conditions following movement of sun, radiation and temperature to keep PV terminal voltage constant at its maximum value. The conventional MPPT methods that has been developed are Perturb and Observer (P and O) and Incremental Conductance (IC) method [12]. In this paper, FLC method as a part of artificial intelligent (AI) is used for determining MPPT in PV panel. The fuzzy set theory is a new method of controlling MPPT in obtaining peak of power point. The MPPT is implemented to obtain MPP operation voltage point faster with less overshoot and it also can minimize voltage fluctuation after MPP has been recognized. The fuzzy inference system (FIS) used in this research are FM and FS respectively.

This paper proposes and compares two methods i.e. FM and FS as MPPT control on PV. The PV is connected to 3P3W of 380 V and 50 Hz on low voltage distribution line through DVR-BES system. The nominal percentage of sag voltage disturbances scenarios is nine disturbances started from 10% to 90%. The swell voltage are the same number started from 110% to 190%. So that the total number of voltage sag/swell scenario using both methods are 18 disturbances scenario. The combination of the DVR-BES-PV system uses two methods connected to a 3P3W system is used in order to maintain the

voltage at sensitive load remain constant. This research are performed on the percentage of sag/swell load voltage, average THD of source voltage, and average THD of load voltage in each MPPT methods and disturbances scenario. Furthermore the results were compared and validated with IEEE 1159 and IEEE 519. This paper is presented as follow. Section 2 describes proposed model of DVR-BES-PV, modelling of PV, UVTG control, sag/swell, harmonics, as well as MPPT-FM and MPPT-FS. Section 3 shows the results and the discusions about performance of percentage and average THD load voltage of sag/swell. Finally, this paper in concluded in Section 4.

2. Research method

2.1 Proposed method

Fig. 1 shows DVR proposed model using BES supplied by PV. The proposed DVR model is located between source or point common coupling (PCC) bus and load bus which it is connected to sensitive load. The PCC bus is then connected to a 3P3W of 380 Volt 50 Hz low voltage distribution line. The DVR consists of injection transformers, filter circuit, active filter series, DC voltage sources, and energy storage. The energy storage which is commonly used is DC link capacitor. The disadvantage of this device has limited energy storage capacity. The series active filter on DVR is controlled by UVTG method to mantain magnitude of voltage between PCC bus and load bus remain constant, balanced, and distortion free. The UVTG method is also used to generate trigger pulses in PWM circuit of six pulses by the active series filter, so as able to generate injection voltage to compensate for sag/swell voltage on load bus. Table 1 shows abbreviation in this paper.

This paper proposes model of DVR-BES system supplied by 0.6 kW PV system. The PV generator produces an output voltage and is an input for the DC/DC boost converter. There are two FLC method proposed in MPPT of PV system i.e. MPPT FM and MPPT-FS respectively. The MPPT-FM/MPPT-FS helps single phase PV generate MPP in DVR-BES-PV system output. The DC output voltage of the PV is relatively low and then it is raised by a DC/DC boost converter at the appropriate voltage level in order to generate active power for BES charging process. The BES has a larger storage capacity than capacitor, otherwise PV are used as an alternative DC voltage source to charge BES when its capacity decreases. The PV also provides active power to compensate for

225

sag/swell voltage. The PV also helps self charging process of BES during uninterrupted conditions (standby mode). Fig. 2 shows PV system using MPPT-FM/MPPT-FS method connected to DC load.

The analysis of the proposed model is investigated by determination of nine sag/swell disturbances scenario on source bus in the 3P3W system using the DVR-BES-PV. Each sag/swell disturbances on source bus uses MPPT-FM and MPPT-FS respectively. The nominal percentage of sag voltage disturbance are 10%, 20%, 30%, 40%, 50%, 60%, 70%, 80%, and 90%. Whereas, swell voltage disturbances are 110%, 120%, 130%, 140%, 150%, 160%, 170%, 180%, and 190%. So that the

total number of sag/swell voltage scenarios using MPPT-FM and MPPT-FS each is 18 disturbances scenario. The combination of DVR-BES-PV system which uses MPPT-FM/MPPT-FS is installed on a 3P3W system to maintain voltage in sensitive load constant. The analysis of this paper is performed on percentage of sag/swell and average THD of load voltage in each MPPT method and disturbances scenario. Then, the results are compared and validated with IEEE 1159 for voltage disturbance standards and IEEE 519 for voltage harmonic standards. Simulation and analysis of this paper using Matlab/Simulink. Parameters for the proposed model are shown in Appendix.
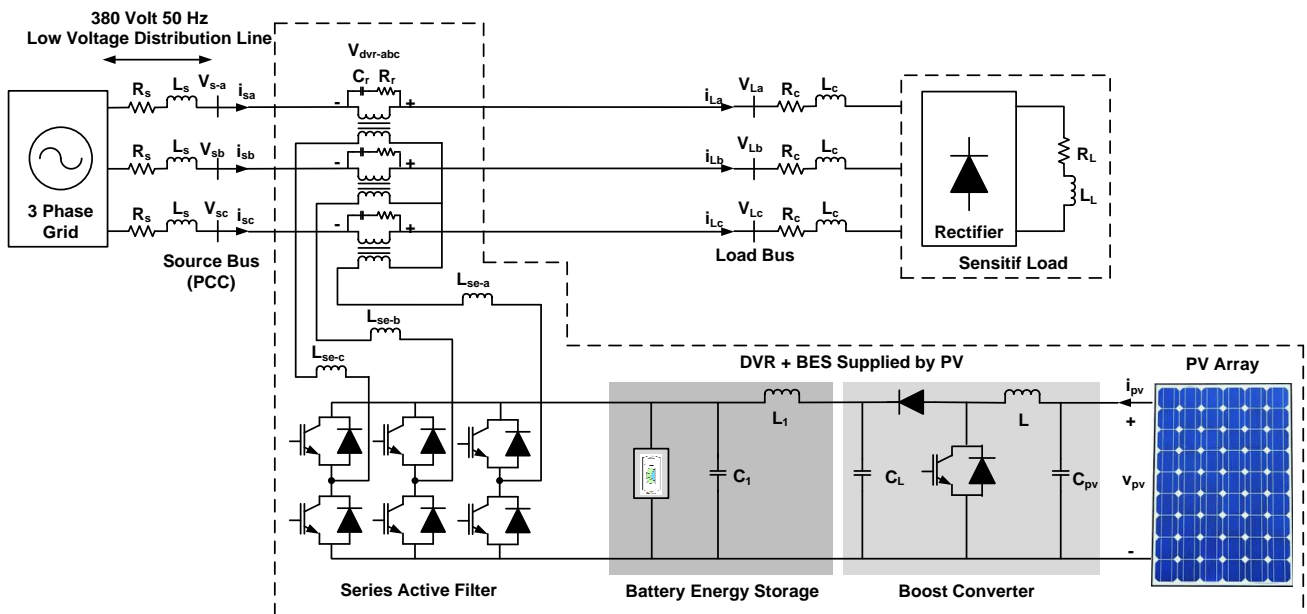

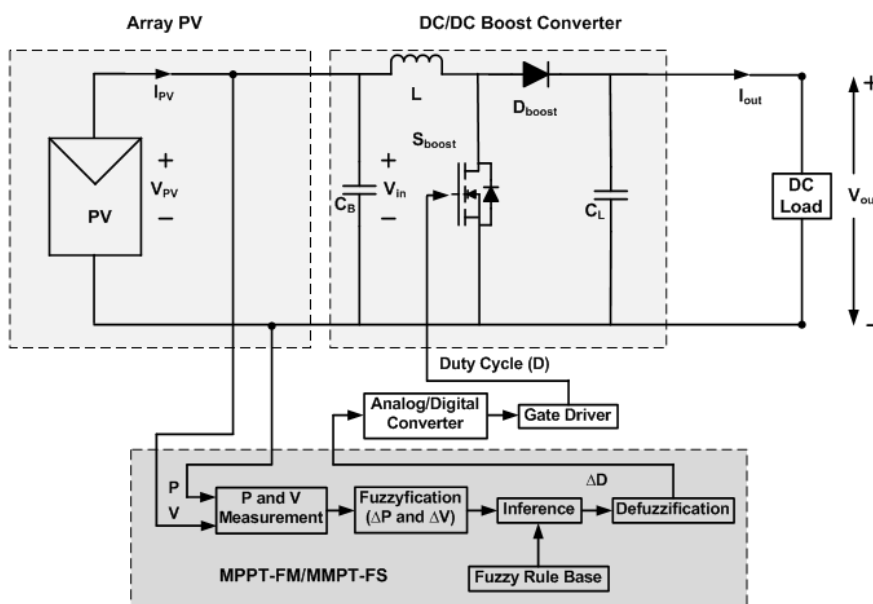Figure. 1 Proposed model of DVR using BES supplied by PV system

Figure. 2 PV system using MPPT-FM/MPPT-FS method connected to DC load

2.2 Modelling of PV array

Fig. 3 shows the equivalent circuit of a solar panel. A solar panel is composed by several PV cells that have series, parallel, or series-parallel external connections [13]. The V-I characteristic of a solar panel is showed in Eq. (1):

$$I = I_{PV} - I_o \left[exp\left(\frac{V+R_SI}{a\,V_t}\right) - 1 \right] - \frac{V+R_SI}{R_P} \qquad (1)$$

Where I_{PV} is the photovoltaic current, I_o is saturated reverse current, 'a' is the ideal diode constant, $V_t = N_SKTq^{-1}$ is the thermal voltage, N_S is the number of series cells, q is the electron charge, K is the Boltzmann constant, T is the temperature of p–n junction, R_S and R_P are series and parallel equivalent resistance of the solar panels. I_{PV} has a linear relation with light intensity and also varies with temperature variations. I_o is dependent on temperature variations. The values of I_{PV} and I_o are calculated as following Eq. (2) and Eq. (3):

$$I_{PV} = (I_{PV,n} + K_I \Delta T) \frac{G}{G_n} I \qquad (2)$$

$$I_o = \frac{I_{SC,n} + K_I \Delta T}{\exp(V_{OC,n} + K_V \Delta T)/aV_t - 1} \qquad (3)$$

In which $I_{PV,n}$, $I_{SC,n}$ and $V_{OC,n}$ are photovoltaic current, short circuit current and open circuit voltage in standard conditions $(T_n = 25\ C\ and\ G_n = 1000\ Wm^{-2})$ respectively. K_I is the coefficient of short circuit current to temperature, $\Delta T = T - T_n$ is the temperature deviation from standard temperature, G is the light intensity and K_V is the ratio coefficient of open circuit voltage to temperature. Open circuit voltage, short circuit current and voltage-current corresponding to the maximum power are three important points of I-V characteristic of solar panel. These points are changed by the variations of atmospheric conditions. By using Eq. (4) and Eq. (5) which are derived from PV model equations, short circuit current and open circuit voltage can be calculated in different atmospheric conditions.
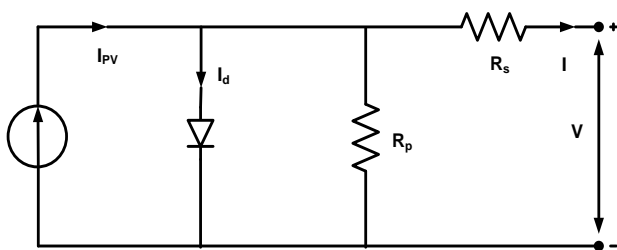

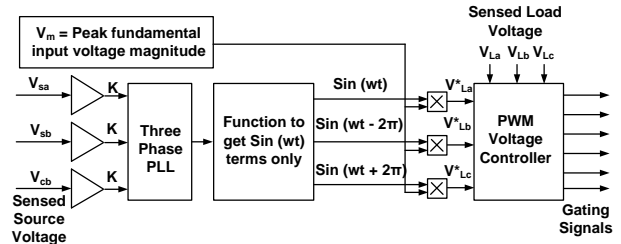Figure. 3 Equivalent circuit of solar panel

Figure. 4 UVTG control of series active filter

$$I_{SC} = (I_{SC} + K_I \Delta T) \frac{G}{G_n} \qquad (4)$$

$$V_{OC} = (V_{OC} + K_V \Delta T) \qquad (5)$$

2.3 UVTG control on series active filter

The main function of series active filter is the sensitive load protection against a number of voltage disturbances at source bus. The control strategy algorithm of the source and load voltage in series active filter is shown in Fig 4. It extracts the UVTG from the distorted input supply. Furthermore, the templates are expected to be ideal sinusoidal signal with unity amplitude. The distorted supply voltages are measured and divided by peak amplitude of fundamental input voltage V_m given in Eq. (6) [14].

$$V_m = \sqrt{\frac{2}{3}(V_{sa}^2 + V_{sb}^2 + V_{sc}^2)} \qquad (6)$$

A three phase locked loop (PLL) is used in order to generate sinusoidal unit vector templates with a phase lagging by the use of sinus function. The reference load voltage signal is determined by multiplying the unit vector templates with the peak amplitude of the fundamental input voltage V_m. The load reference voltage $(V_{La}^*,\ V_{Lb}^*,\ V_c^*)$ is then compared to the sensed load voltage $(V_{La},\ V_{Lb},\ V_{Lc})$ by a PWM controller used to generate the desired trigger signal on series active filter.

2.4 Voltage sag/swell

The voltage sag is defined as a decrease in the value of rms voltage between 10-90% which goes on from one half cycle to one minute. The voltage sag can affect to the phase or amplitude. The most voltages sag occurs caused by a single phase to ground short circuit. An unbalanced short circuit can trigger an unbalanced phase and shift it from its nominal value. The starting of motor with high power also can generate voltage sag. The amplitude of the voltage sag depends on several factors i.e. type, location, and impedance disturbance. The voltage sag in each busbar is different depends on

location of disturbance. The duration of sag is determined by duration of protection clearing time i.e. the extent to which voltage sag is able to be removed. The voltage swell is an increase in source rms voltage in short time intervals whose value ranges from 1.1 pu to 1.8 p.u from nominal source voltage. Although the duration time of voltage sag/swell is short, the interference can affect sensitive loads such as the computers, the programmable logic controllers (PLCs) and the variable speed drives (VSDs) on motor and simultaneously reducing efficiency of these devices. The DVR is a special power electronics device used to reduce voltage sag/swell. The DVR is able to protect sensitive loads that may be drastically affected by voltage fluctuations in the distribution system [15]. The recommended standard of practice on monitoring voltage sag/swell as the part of electric power quality parameters is IEEE 1159-1995 [16]. This standard presents definition and table of voltage sag/swell base on categories (instantaneous, momentary, temporary) typical duration, and typical magnitude. The typical residential utility power after sag/swell disturbance is in the range of +/-5% from the nominal value [17]. The percentage of voltage sag is formulated in Eq. (7) [18] and with the same procedure, the authors propose Eq. (8) for percentage of voltage swell.

$$Sag(\%) = \frac{Vpre\ sag - Vsag}{Vpre\ sag} \qquad (7)$$

$$Swell(\%) = \frac{|Vpre\ swell - Vswell|}{Vpre\ swell} \qquad (8)$$

2.5 Voltage harmonics

Harmonics of power systems are low frequency phenomena characterized by waveform distortion, which introduces harmonic frequency components. Voltage and current harmonics have an undesirable effect on the operation of power systems and power system components [19]. In general, current and voltage waves form pure sinusoidal. The prominent problem in the distribution system is voltage harmonics waves generated by source of a distorted power system and non-sinusoidal currents due to the presence of sensitive/ non-linear loads. Harmonics is a periodic steady state wave that occurs due to interaction between sine wave forms at fundamental frequency with other waves where the wave is a multiple of fundamental frequency. The most common harmonics index, which is related to voltage waveforms, is THD which is defined as root mean square (rms) value of harmonics expressed as a percentage of fundamental component, as stated in

Eq. 9 [20].

$$THD_V = \frac{\sqrt{\sum_{n=2}^{N} V_n^2}}{V_1} \times 100\% \qquad (9)$$

Where V_n is a single frequency r.m.s voltage at the harmonic n, N is maximum harmonic order to be considered, and V_1 is fundamental line to neutral rms voltage. THD standard most often used in electric power systems is IEEE 519. According to IEEE 519, voltage harmonic distortion in power systems 69 kV and below is limited to 5% THD with each individual harmonics limited by 3% [21].

2.6 MPPT-FM and MPPT-FS

The initial research is to determine value of duty cycle (D) with a variable step to control DC/DC boost converter circuit using MPPT algorithm on PV power output. MPPT has been developed. MPPT searches for the maximum power independent based on environmental conditions, follows changes in solar radiation and temperature, as well as maintains PV output voltage remains constant at maximum value. In this paper FLC method is proposed as MPPT control in PV panel. The fuzzy inference system (FIS) used in this research are FM and FS respectively.

The difference between FM and FS is how to determine the output crips generated from fuzzy inputs. The FM uses a technique of fuzzy output defuzzification, while FS uses weighted average to compute output crips. The ability to express and interpret on FM output is lost in FS, because the consequents of rules are not fuzzy. However FS has a better processing time because weighted average replaces defuzzification process which takes a relatively long time. Because the basic nature of rules that can be interpreted and intuitively, FM can be widely used especially for decision support applications. The FM has an output membership functions (MFs), while FS has no output MFs [22].

MPPT-FLC with FM and FS FIS method respectively is applied by determining input variables, namely fuzzy control output of voltage *(V)* and power *(P)* of PV, seven linguistic variables fuzzy sets, fuzzy operating system block (fuzzification, fuzzy rule base, and defuzzification), function delta voltage *(ΔV)* and delta power (ΔP) during fuzzification, a table fuzzy rule base, crisp values to determine delta duty-cycle *(ΔD)* in defuzzification phase with variable step to control DC/DC boost converter circuit. Fig. 5 shows MPPT-FLC using Mamdani/Sugeno FIS.
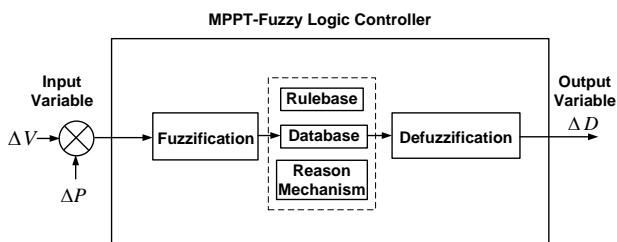
Figure. 5 MPPT-fuzzy Mamdani/MPPT fuzzy Sugeno

In the fuzzification phase shown in Fig. 5, a number of input variables ΔV and ΔP are calculated and converted into a linguistic variable based on the subset ΔV and ΔP called MFs. The input of ΔV and ΔP are designed to use seven variable fuzzy sets i.e. *PB* (Positive Big), *PM* (Positive Medium), PS (Positive Small), Z (Zero), *NS* (Negative Small), *NM* (Negative Medium), and *NB* (Negative Big). The delta voltage *(ΔV)* and delta power *(ΔP)* are proposed as input variables. While output variable is duty cycle change value *(ΔD)*. The input MFs of MPPT-FM and MPPT-FS are same in Max-Min but output MFs of them is different. MPPT-FM has MFs in Max-Min but MPPT-FS has MFs in constant [0,1]. The MFs of MPPT-FM input and output are presented with triangular and trapezoidal. The value of *ΔV* range from -10 to 10, ΔP from -10 to 10, and *ΔD* from -5 to 5. The output MFs of MPPT-FS is *ΔD* [0,1] from -5 to 5. The delta voltage and delta power for MPPT-FM/MPPT-FS are showed in Fig. 6 and Fig. 7. While delta duty cycle for MPPT-FM and MPPT-FS are showed in Fig. 8 and Fig. 9. Fig. 10 and Fig. 11 show surface view of MFs of MPPT-FM and MPPT-FS respectively.
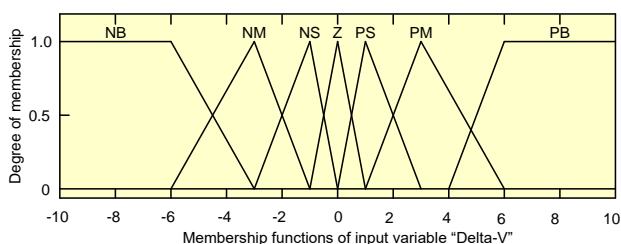

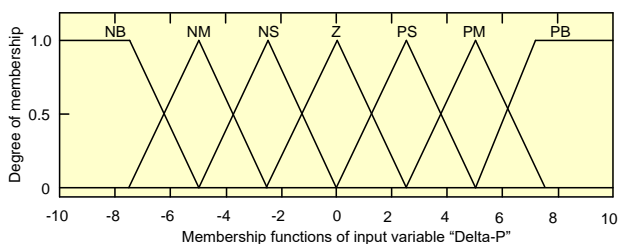Figure. 6 Input MFs of MPPT-FM/MPPT-FS (ΔV)

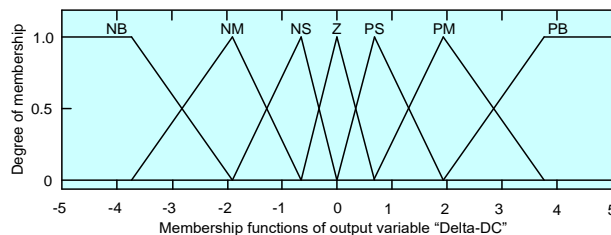Figure. 7 Input MFs of MPPT-FM/MPPT-FS (ΔP)

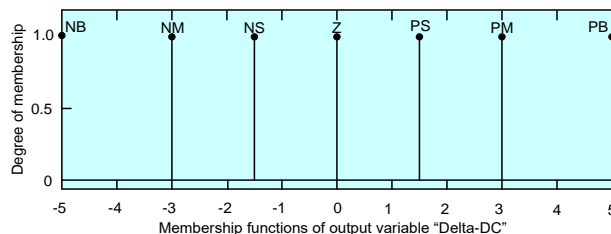Figure. 8 Output MFs of MPPT-FM (ΔD)
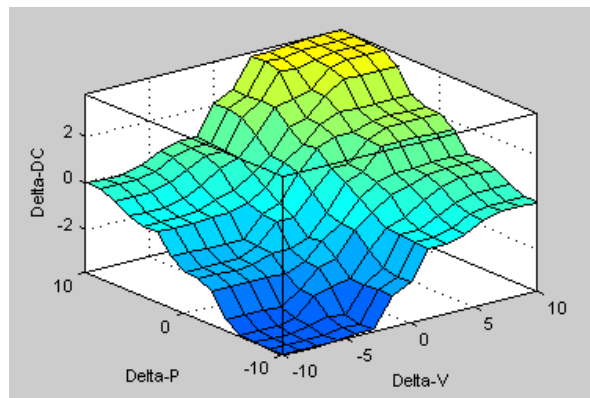

Figure. 9 Output MFs of MPPT-FS (ΔD)

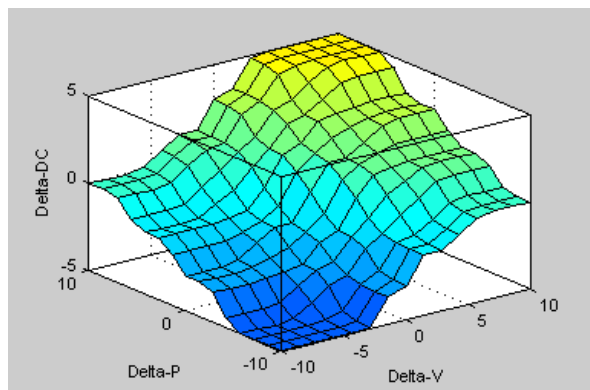Figure 10. MFs surface view of MPPT-FM

Figure. 11 MFs surface view of MPPT-FS

The limit of input and output MFs, determined by prior knowledge of parameter variations. The FIS consists of three parts, namely rule base, database, and reasoning mechanism as shown in Fig. 5. After determine ΔV and ΔP, then both are converted into linguistic variables and use them as input functions for MPPT-FM/MPPT-FS. The output value is ΔD is generated using block inference and fuzzy rules as shown in Table 2.

Table 2. Fuzzy Rule Base

ΔV / ΔP	NB	NM	NS	Z	PS	PM	PB
PB	Z	PS	PS	PM	PM	PB	PB
PM	NS	Z	PS	PS	PM	PM	PB
PS	NS	NS	Z	PS	PS	PM	PM
Z	NM	NS	NS	Z	PS	PS	PM
NS	NM	NM	NS	NS	Z	PS	PS
NM	NB	NM	NM	NS	NS	Z	PS
NB	NB	NB	NM	NM	NS	NS	Z

Finally defuzzyfication block operates to change value of ΔD is raised from linguistic variables into numeric variables back. Then, the numeric variables become an inputs signal for the IGBT switch of DC/DC boost converter to determine MPPT value for PV connected to DVR-BES and 3P3W system.

3. Result and discussion

The proposed model is analyzed through the determination of nine sag/swell voltage disturbance scenarios on source bus of 3P3W using DVR-BES-PV system. Each disturbances scenario on source bus uses MPPT-FM and MPPT-FS Methods. The nominal percentage of voltage sag/swell disturbances are nine so the total are 18 scenarios. The combination of DVR-BES-PV system circuit

with MPPT-FM/MPPT-FS method is used to maintain voltage at sensitive load bus. By using Matlab/Simulink, the model then is run based on desired scenario to obtain source voltage (V_S) and load voltage (V_L) curves, percentage of voltage sag *(%)*, and percentage of voltage swell *(%)* using Eq. (7) and Eq. (8) [18] with average pre-sag/swell voltage equal as 310,234 V.

Furthermore, source voltage THD and load voltage THD in each phase are determined by using fast fourier transform (FFT) analysis base on the curve with Eq. 9 [20]. Then, the average THD of source voltage and load voltage are calculated from both of THD values in each phase previously. The total duration simulation occurs for 0.2 seconds with duration of sag/swell voltage disturbance between 0.06-0.14 second. The THD voltage in each phase is determined for one cycle starting at t = 0.1 seconds. The next step, percentage of sag/swell load voltage *(%)*, average THD of source voltage *(%),* and average THD of load voltage (%) on each MPPT control methods and scenarios are presented in Table 3. By using the same procedure for swell voltage disturbances, the parameters and simulation results are also shown in Table 4. Fig. 12 and Fig. 13 present performance of sag and swell voltage using DVR-BES-PV with MPPT-FM/MPPT-FS.

Table 3. Percentage of voltage sag and voltage harmonics

Sag Scn	Source Voltage (Volt)			Load Voltage (Volt)			Sag (%)	Source Voltage THD (%)				Load Voltage THD (%)			
	A	B	C	A	B	C		A	B	C	Avg	A	B	C	Avg
MPPT Fuzzy Mamdani															
10%	278.3	278.3	278.3	310.2	310.2	310.2	**0.011**	0.21	0.21	0.21	0.21	0.37	0.37	0.37	**0.370**
20%	247.3	247.3	247.3	310.2	310.2	310.2	**0.011**	0.23	0.23	0.23	0.23	0.37	0.37	0.37	**0.370**
30%	216.2	216.2	216.2	310.2	310.3	310.2	**0.011**	0.27	0.27	0.27	0.27	0.38	0.36	0.36	**0.367**
40%	185.2	185.2	185.2	310.2	310.2	310.2	**0.011**	0.31	0.31	0.31	0.31	0.37	0.36	0.35	**0.360**
50%	154.2	154.2	154.2	310.2	309.9	309.9	**0.075**	0.37	0.37	0.38	0.37	0.38	0.42	0.41	**0.404**
60%	123.2	123.2	123.2	310.1	307.4	307.4	**0.623**	0.47	0.46	0.47	0.47	0.38	2.09	2.07	**1.514**
70%	92.13	92.16	92.17	309.9	301.7	302.2	**1.816**	0.61	0.60	0.62	0.61	0.43	5.35	5.27	**3.684**
80%	61.11	61.14	61.18	308.2	295.6	293.4	**3.600**	0.88	0.89	0.94	0.91	2.46	8.51	8.00	**6.324**
90%	30.10	30.13	30.19	305.6	288.4	283.1	**5.759**	1.72	1.80	1.90	1.81	6.35	13.14	11.46	**10.32**
MPPT Fuzzy Sugeno															
10%	278.3	278.3	278.3	310.2	310.2	310.2	**0.011**	0.21	0.21	0.21	0.21	0.37	0.37	0.37	**0.370**
20%	247.3	247.3	247.3	310.2	310.2	310.2	**0.011**	0.23	0.23	0.23	0.23	0.37	0.37	0.37	**0.370**
30%	216.2	216.2	216.2	310.2	310.2	310.2	**0.011**	0.27	0.27	0.27	0.27	0.38	0.38	0.36	**0.374**
40%	185.2	185.2	185.2	310.2	310.2	310.2	**0.011**	0.31	0.31	0.31	0.31	0.38	0.36	0.34	**0.360**
50%	154.2	154.2	154.2	310.1	310.0	309.9	**0.076**	0.37	0.37	0.38	0.37	0.38	0.37	0.39	**0.380**
60%	123.2	123.2	123.2	310.0	307.7	307.6	**0.581**	0.47	0.46	0.47	0.47	0.40	1.75	1.73	**1.294**
70%	92.13	92.16	92.17	309.9	301.6	302.2	**1.826**	0.61	0.60	0.63	0.61	0.44	5.41	5.34	**3.730**
80%	61.11	61.14	61.18	308.1	295.6	293.5	**3.600**	0.88	0.89	0.94	0.91	2.23	8.52	2.23	**4.327**
90%	30.10	30.13	30.19	304.9	288.6	283.5	**5.770**	1.71	1.80	1.88	1.80	6.38	12.87	11.17	**10.14**

Table 4. Percentage of voltage swell and voltage harmonics

Swell Scn	Source Voltage (Volt)			Load Voltage (Volt)			Swell (%)	Source Voltage THD(%)				Load Voltage THD (%)			
	A	B	C	A	B	C		A	B	C	Avg	A	B	C	Avg
MPPT Fuzzy Mamdani															
110%	340.3	340.3	340.3	310.3	310.3	310.3	**0.021**	0.17	0.17	0.17	0.17	0.37	0.37	0.37	**0.370**
120%	371.4	371.4	371.4	310.3	310.3	310.4	**0.032**	0.16	0.16	0.16	0.16	0.37	0.37	0.37	**0.370**
130%	402.4	402.4	402.4	310.4	310.4	310.4	**0.054**	0.14	0.14	0.14	0.14	0.37	0.37	0.37	**0.370**
140%	433.4	433.4	433.4	310.4	310.4	310.4	**0.054**	0.13	0.13	0.13	0.13	0.37	0.37	0.35	**0.364**
150%	464.5	464.5	464.5	310.4	310.3	310.4	**0.042**	0.12	0.12	0.12	0.12	0.38	0.37	0.35	**0.367**
160%	495.5	495.5	495.5	310.4	310.4	310.5	**0.064**	0.12	0.12	0.12	0.12	0.35	0.37	0.35	**0.357**
170%	526.5	526.5	526.5	310.4	310.4	310.6	**0.075**	0.11	0.11	0.11	0.11	0.36	0.37	0.38	**0.370**
180%	557.5	557.5	557.5	310.5	310.7	311.1	**0.172**	0.10	0.10	0.10	0.10	0.39	0.41	0.48	**0.427**
190%	588.6	588.6	588.6	311.4	312.8	314.8	**0.892**	0.10	0.10	0.10	0.10	1.16	1.72	1.90	**1.594**
MPPT Fuzzy Sugeno															
110%	340.3	340.3	340.3	310.3	310.3	310.3	**0.021**	0.17	0.17	0.17	0.17	0.37	0.37	0.36	**0.367**
120%	371.4	371.4	371.4	310.3	310.4	310.4	**0.043**	0.16	0.16	0.16	0.16	0.37	0.36	0.37	**0.367**
130%	402.4	402.4	402.4	310.3	310.4	310.2	**0.021**	0.14	0.14	0.14	0.14	0.37	0.37	0.35	**0.364**
140%	433.4	433.4	433.4	310.3	310.3	310.3	**0.021**	0.13	0.13	0.13	0.13	0.37	0.37	0.34	**0.360**
150%	464.5	464.5	464.5	310.4	310.3	310.4	**0.043**	0.12	0.12	0.12	0.12	0.37	0.37	0.35	**0.363**
160%	495.5	495.5	495.5	310.4	310.4	310.5	**0.065**	0.12	0.12	0.12	0.12	0.37	0.37	0.36	**0.367**
170%	526.5	526.5	526.5	310.4	310.4	310.6	**0.075**	0.11	0.11	0.11	0.11	0.37	0.37	0.39	**0.377**
180%	557.5	557.5	557.5	310.5	310.8	311.3	**0.204**	0.10	0.10	0.10	0.10	0.39	0.58	0.69	**0.554**
190%	588.6	588.6	588.5	311.3	313.4	315.9	**1.064**	0.10	0.10	0.10	0.10	1.49	2.11	2.66	**2.087**

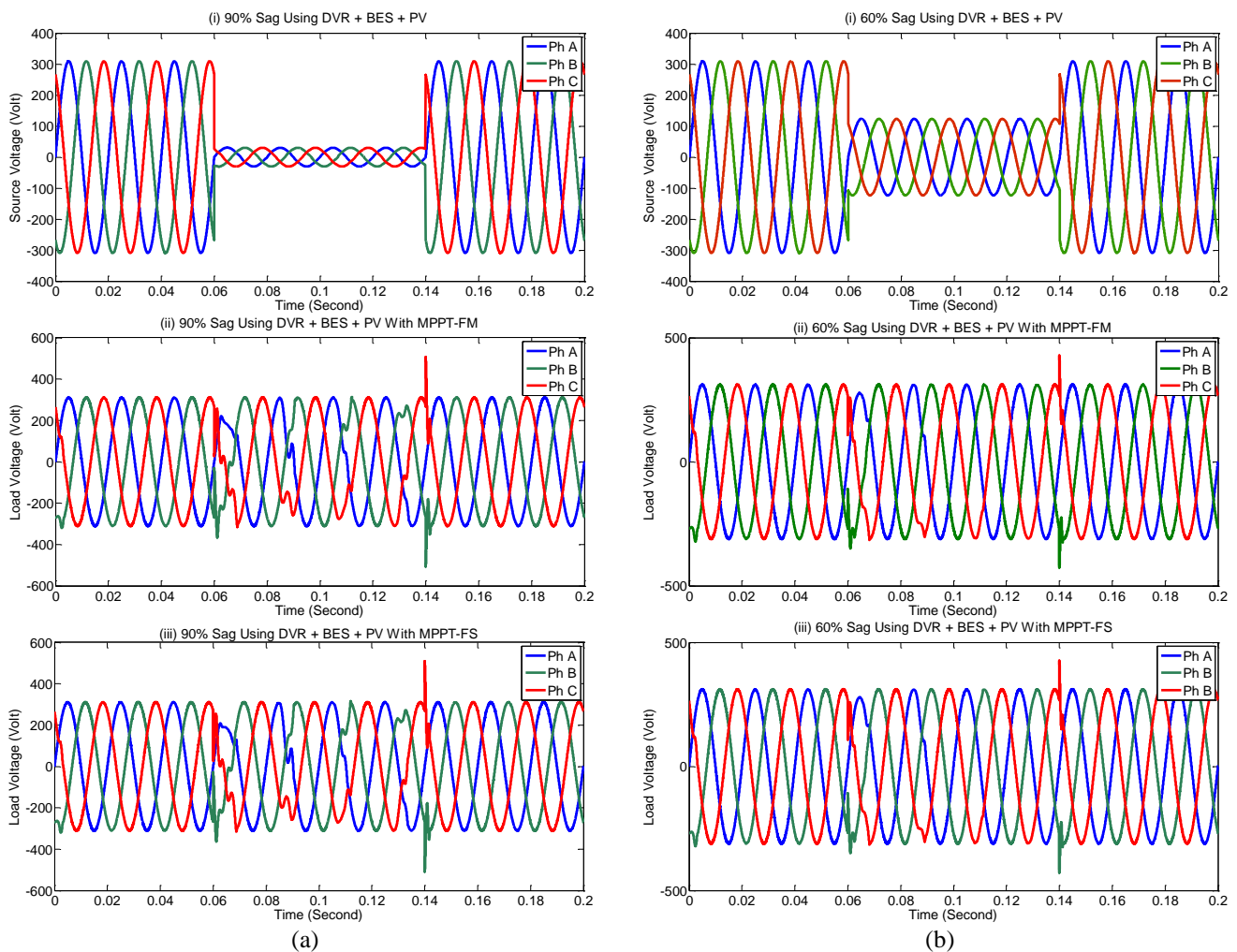(a)   (b)

Figure. 12 Performance of sag using DVR-BES-PV with MPPT-FM/MPPT-FS: (a) 90% sag using DVR-BES-PV system and (b) 60% sag using DVR-BES-PV system
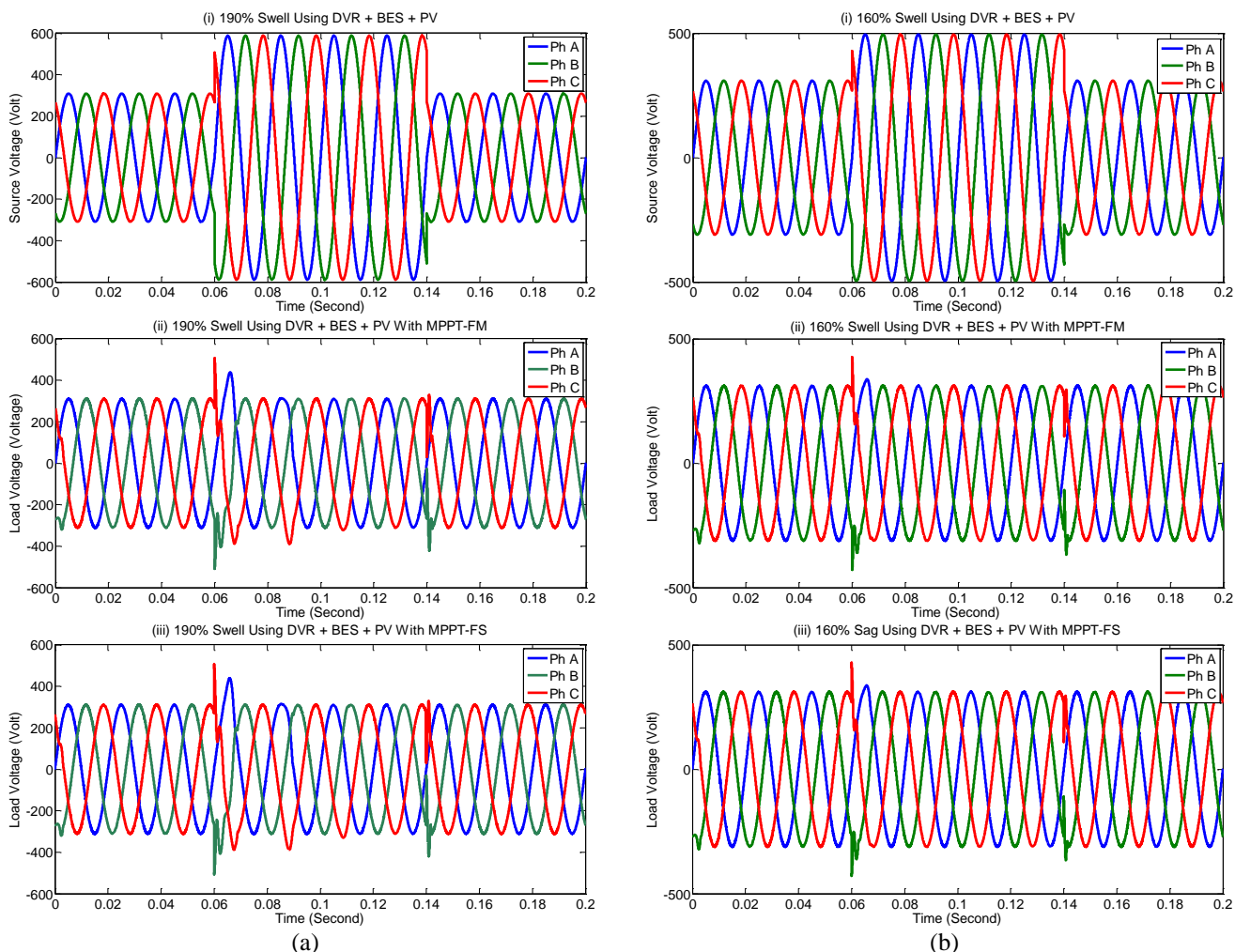
Figure. 13 Performance of swell using DVR-BES-PV with MPPT-FM/MPPT-FS: (a) 190% swell using DVR-BES-PV system and (b) 160% swell using DVR-BES-PV system
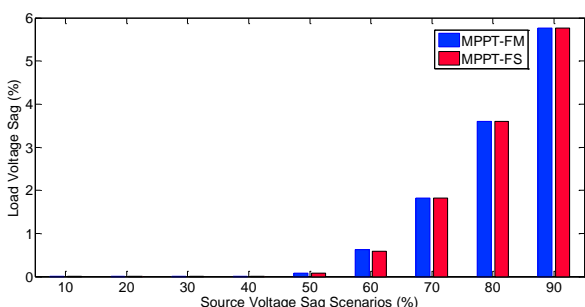

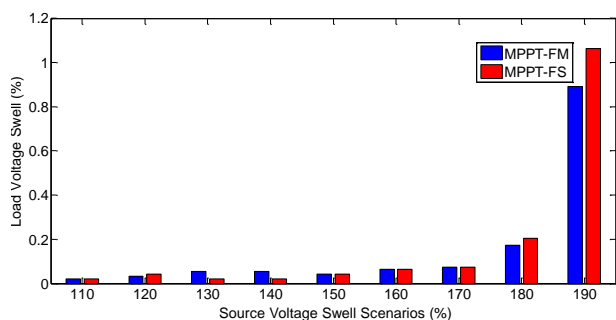Figure. 14 Percentage of load voltage sag

Figure. 15 Percentage of load voltage swell

Fig. 14 and Fig. 15 show percentage of load voltage sag and load voltage swell in nine disturbances scenario using DVR-BES-PV system with MPPT-FM/MPPT-FS.

Fig. 12.a.i. shows that in 90% sag on source bus, DVR-BES-PV system using MPPT-FM at t = 0.06 s to t = 0.14 s, average of V_S falls from 310,234 V to 30.14 V. During the disturbance, PV is able to generate power to charge BES and injecting full average of compensation voltage through injection transformer by series active filter in DVR so that average of V_L in Fig. 12.a.(ii) remains stable at 292.334 V and then results percentage of sag and average THD voltage in load bus of 5.759% and 10.32%. By the same procedure, implementation of MPPT-FS on DVR-BES-PV system results percentage sag and average THD voltage in load bus as 5.770 % and 10.14% as shown in Fig. 12.a.(iii). Furthermore, for 10% to 80% voltage sag disturbances, the nominal of percentage of sag and average THD of load voltage are shown in Table 3.

Fig. 13.a.(i) shows that in 190% swell on source bus, DVR-BES-PV system using MPPT-FM at t = 0.06 s to t = 0.14 s, average of V_S rises from 310,234 V to 588.6 V. During the disturbance, PV is able to generate power to charge BES and injecting full average of compensation voltage with opposite polarities through injection transformer by series active filter in DVR so that average of V_L in Fig. 13.a.(ii) remains stable at 313 V and then results percentage of sag and average voltage THD in load bus of 0.892% and 1.594 %. By the same procedure, implementation of MPPT-FS on DVR-BES-PV system results percentage swell and average THD voltage in load bus as 1.064 % and 2.087 % as shown in Fig. 13.a.(iii). Furthermore, for 110% to 180% voltage swell disturbances, the nominal of percentage of swell and average THD of load voltage are shown in Table 4.

Table 3 and Fig. 14 show that for voltage sag disturbances scenario on source bus, the 3P3W system using DVR-BES-PV with MPPT-FM/MPPT-FS, the higher percentage drop of voltage sag on source bus, then percentage of voltage sag on load bus is also higher. The MPPT-FM is able to result a smaller percentage of voltage sag than MPPT-FS. In 90% voltage sag on source bus, MPPT-FM is able to result percentage of load voltage sag of 5.759%, lower than MPPT-FS of 5.770%. Reviewed from harmonics mitigation, MPPT-FM is able to result an average voltage THD higher than MPPT-FS. In 90% voltage sag on source bus, MPPT-FM is able to results an average THD of load voltage of 10.32%, higher than MPPT-FS of 10.14%.

Table 4 and Fig. 15 show that for voltage swell disturbances scenario on the source bus in 3P3W system using DVR-BES-PV with MPPT-FM/MPPT-FS method, the higher percentage increase in voltage swell on source bus, then percentage of voltage swell on load bus is also higher. The MPPT-FM method is able to result a smaller percentage of voltage swell than MPPT-FS. In 190% swell voltage on source bus, MPPT-FM method is able to result a percentage of load voltage swell of 0.892%, lower than MPPT-FS of 1.064%. Reviewed from harmonics mitigation, MPPT-FM method is able to result an average of THD voltage smaller than the MPPT-FS. In 190% voltage swell on source bus, MPPT-FM method is able to result an average THD of load voltage of 1.594%, smaller than the MPPT-FS of 2.087%. The average THD of load voltage using MPPT-FM/MPPT-FS in nine swell voltage disturbances scenario on source bus is smaller than voltage sag and its value already has met the limits prescribed in IEEE 519.
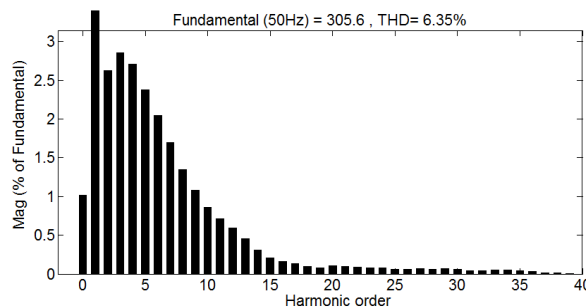

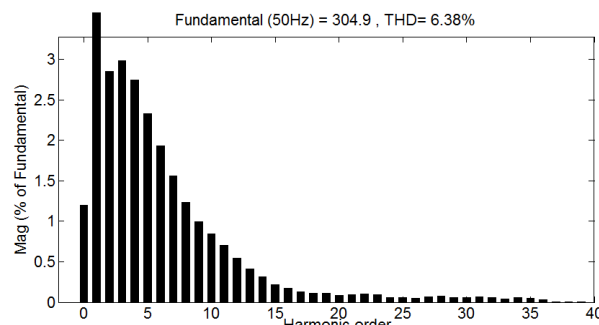Figure. 16 Spectra of harmonic load voltage on phase A for 90% sag using DVR-BES-PV with MPPT-FM

Figure. 17 Spectra of harmonic load voltage on phase A for 90% sag using DVR-BES-PV with MPPT-FS
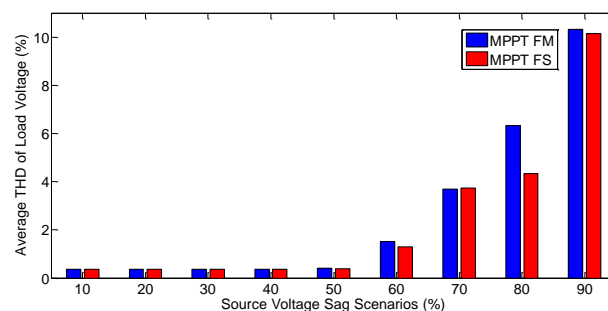

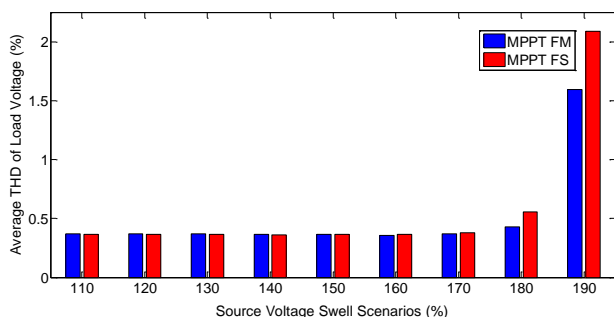Figure. 18 Performance of average THD load voltage for voltage sag

Figure. 19 Performance of average THD load voltage for voltage swell

Fig. 16 and Fig. 17 show spectra of harmonic load voltage on phase A for 90% sag using MPPT-FM and MPPT-FS.

Fig. 18 shows performance of an average THD of load voltage in nine voltage sag disturbances scenario using DVR-BES-PV system with MPPT-

FM/MPPT-FS. Fig. 19 also shows the same performance for voltage swell.

Fig. 18 shows that in the 3P3W system using DVR-BES-PV with MPPT-FM/MPPT-FS method, the higher percentage drop of voltage sag on source bus, then average THD of load voltage is also higher. The MPPT-FM method is able to result an average THD of load voltage THD higher than MPPT-FS method. Fig. 19 shows that in the 3P3W system using DVR-BES-PV with MPPT-FM/MPPT-FS method, the higher percentage increase of voltage swell on source bus, then an average THD of load voltage is also higher. The MPPT-FM method is able to result an average THD of load voltage smaller than MPPT-FS method. The average THD of load voltage using MPPT-FM/MPPT-FS in nine swell voltage disturbances on the source bus, is smaller than sag voltage and its value has met the limits prescribed in IEEE 519.

4. Conclusion

Comparative performance analysis between MPPT-FM and MPPT-FS as controller on PV output power using DVR-BES-PV system connected to 3P3W distribution network have been discussed. The combination of DVR-BES-PV system using two methods is used in order to mitigate voltage sag/swell and harmonics on load bus. The UVTG is used to control series active filter in DVR when it injects compensation voltage during voltage sag/swell disturbance. The PV is used as an alternative DC voltage source to charge BES when its capacity decreases and provides active power needed to compensate for sag/swell.

In nine sag/swell disturbances scenario, the higher percentage drop of sag/increase of swell voltage on source bus, then percentage of sag/swell voltage on load bus is also higher. In the same disturbances and scenarios, the higher percentage drop of sag/increase of swell voltage on source bus, then average THD of load voltage is also higher. The MPPT-FM is able to produce a smaller percentage of voltage sag/swell than MPPT-FS. In nine disturbances scenario, both of MPPT-FM and MPPT-FS are able to result percentage of sag/swell on load voltage under IEEE 1159. In voltage sag, MPPT-FM is able to result an average THD of load voltage THD higher than MPPT-FS. Otherwise in voltage swell, MPPT-FM is able to result an average THD of load voltage smaller than MPPT-FS. The average THD of load voltage using MPPT-FM/MPPT-FS in nine voltage swell disturbances scenario on source bus, is smaller than voltage sag

and its value has met the limits prescribed in IEEE 519.

Nevertheless, the average THD of load voltage in 90% sag scenario (deep voltage sag) using MPPT-FM/MPPT-FS has exceeded the limit prescribed in IEEE 519. The implementation of advanced Fuzzy Method i.e. Fuzzy Type 2, Fuzzy Sliding Mode, or both combination for controlling MPPT on PV connected to DVR-BES system is proposed as future work to overcome this problem.

Acknowledgments

Appendix

Three phase grid: RMS voltage = 380 volt (L-L), frequency = 50 Hz, line source impedance R_s = 0.1 Ohm, line source inductance L_s = 15 mH; Series active filter: series inductance L_{se} = 0.015 mH, Series transformer: kVA rating = 10 kVA, frequency 50 Hz, N_1/N_2 = 1:1; Sensitive Load: load resistance R_L = 60 Ohm, load inductance L_L = 0.15 mH, line load resistance R_c = 0.4 Ohm, line load inductance L_c = 15 mH; Battery energy storage: Type = nickel metal hibrid, DC voltage = 650 V, capacity = 200 Ah, initial SOC, 100%, inductance L_1 = 6 mH, capacitance C_1 = 200 µF; PV array active power = 0.6 kW, temperature = 25^0 C, irradiance = 1000 W/m^2; MPPT-FM model: FIS = mamdani, composition = max-min; input membership function: delta voltage (ΔV) = trapmf, trimf, delta power (ΔP) = trapmf, trimf; output membership function: delta duty cycle (ΔD) = trapmf, trimf, defuzzyfication = centroid; MPPT-FS model: FIS = sugeno, composition = max-min; input membership function: delta voltage (ΔV) = trapmf, trimf, delta power (ΔP) = trapmf, trimf; output membership function: delta duty cycle (ΔD) = constant [0,1], defuzzyfication = wtaver.

References

[1] V.S. Karale, S.S. Jadhao, M. Tasare, and G.M. Dhole, "UVTG based Dynamic Voltage Restorer for Mitigation of Voltage Sag", In: *Proc. of International Conf. on Computing*

Communication Control and automation, pp. 1-6, 2016.

[2] A. M. Munoz, D. Oterino, M. Gonzalez, F.A. Olivencia, and J. J. Gonzalez-de-la-Rosa, "Study of Sag Compensation with DVR", In: *Proc. Mediterranean Electrotechnical Conf.*, pp. 990-993, 2006.

[3] A. Kumar, N. S. Pal, and M. A. Ansari, "Mitigation of Voltage Sag/Swell and Harmonics using Self-Supported DVR", In: *Proc. International Conf. on Power Electronics, Intelligent, Control and Energy Systems*, pp. 1-5, 2016.

[4] N. Prakash, J. Jacob, and V. Reshmi, "Comparison of DVR performance with Sinusoidal and Space Vector PWM techniques", In: *Proc. Annual International Conference on Emerging Research Areas: Magnetics, Machines and Drives,* Kottayam, pp. 1-6, 2014.

[5] A. M. Rauf and V. Khadkikar, "Integrated Photovoltaic and Dynamic Voltage Restorer System Configuration", *IEEE Transactions on Sustainable Energy,* Vol. 6, No. 2, pp. 400-410, 2015.

[6] M. Ramasamy and S. Thangavel, "Photovoltaic Based Dynamic Voltage Restorer with Energy Conservation Capability using Fuzzy Logic Controller", In: *Proc. of International Conf. on Emerging Trends in Science, Engineering and Technology*, pp. 485-492, 2012.

[7] S. Babu and N. Kamaraj, "Performance Investigation of Dynamic Voltage Restorer using PI and Fuzzy Controller", In: *Proc. International Conf. on Power, Energy and Control*, pp. 467-472, 2012.

[8] M. M. Far, E. Pashajavid, and A. Ghosh, "Power Capacity Management of Dynamic Voltage Restorers Used for Voltage Sag and Unbalance Compensation", In: *Proc. Australasian Universities Power Eng. Conf.*, pp. 1-6, 2017.

[9] A. Teke, K. Bayindir, and M. Tumay, "Fast sag/swell detection method for fuzzy logic controlled dynamic voltage restorer", *IET Generation, Transmission and Distribution,* Vol. 4 , No. 1, pp. 1-12, 2010.

[10] E. Babaei, F. M. Shahir, S. D. Tabrizi, and M. Sabahi, "Compensation of Voltage Sags and Swells using Photovoltaic Source Based DVR", In: *Proc. International Conf. on ElectricalEngineering/Electronics, Computer, Telecommunications and Information Tech.*, pp. 903-906, 2017.

[11] R. Dharavath, I. J. Raglend, and A. Manmohan, "Implementation of Solar PV- Battery Storage with DVR for Power Quality Improvement", In: *Proc. of International Conf. on Innovations in Power and Advanced Computing Technologies, Innovations in Power and Advanced Computing Technologies*, pp. 1-5, 2017.

[12] A. Amirullah, A. Kiswantono, O. Penangsang, and A. Soeprijanto, "Transient Power Quality Performance of Multi Photovoltaics using MPPT P and O/MPPT Fuzzy", *Telkomnika*, Vol.16, No.6, pp.2967-2979, 2018.

[13] A. Amirullah and A. Kiswantono, "Power Quality Enhancement of Integration Photovoltaic Generator to Grid under Variable Solar Irradiance Level using MPPT-Fuzzy", *International Journal of Electrical and Computer Engineering,* Vol. 6, No. 6, pp. 2629-2642, 2016.

[14] Y. Bouzelata, E. Kurt, R. Chenni, and N. Altın, "Design and Simulation of Unified Power Quality Conditioner Fed by Solar Energy", *International Journal of Hydrogen Energy* Vol. 40, pp. 15267-15277, 2015

[15] M. Zadehbagheri, R. Ildarabad, and M.B. Nejad, "Modeling and Simulation of Dynamic Voltage Restorer for Voltage Sag/Swell Compensation in Power Distribution Networks: A Review", *International Journal of Mechatronic, Electrical, and Computer Technology,* Vol. 5(16), pp. 2258-2275, 2015.

[16] R.P. Bingham, "Sags and Swells", *Technology and Products Dranetz-BMI 1000,* New Durham Road, pp. 3, 1998.

[17] *1159-1995-IEEE Recommended Practice for Monitoring Electric Power Quality,* New York, USA, 2009.

[18] A.O. Al-Mathnani, A. Mohamed, M. Alauddin, and M. Ali, "Photovoltaic Based Dynamic Voltage Restorer For Voltage Sag Mitigation", In: *Proc. of 5th Student Conf. on Research and Development*, pp. 1-6, 2007.

[19] C. Sankaran, *Power Quality,* CRC Press LLC, New-York, USA, 2002.

[20] J. Arrilaga, B. C. Smith, N. R. Watson, and A. R. Wood, *Power System Harmonics,* Chicester USA: John Wiley and Son Publisher, 2003.

[21] T. M. Bloming, P. E. and D. J. Carnovale, P.E., *Application of IEEE Standard 519-1992 Harmonic Limits,* Presented at The 2005 IEEE IAS Pulp and Paper Industry Conference in Appleton, WI, 2005.

[22] K. Arshdeep and K. Amrit, "Comparison of Mamdani-Type and Sugeno-Type Fuzzy Inference Systems for Air Conditioning System", *International Journal of Soft*

235

Computing and Engineering, Vol. 2, No. 2, 2012.